

Fluoride Interferes with the Sperm Fertilizing Ability via Downregulated SPAM1, ACR, and PRSS21 Expression in Rat Epididymis

Yu Liu, Chen Liang, Yan Gao, Shanshan Jiang, Yuyang He, Yongli Han, Ali Olfati, Ram Kumar Manthari, Jundong Wang, and Jianhai Zhang*

Shanxi Key Laboratory of Ecological Animal Science and Environmental Veterinary Medicine, College of Animal Science and Veterinary Medicine, Shanxi Agricultural University, Taigu, Shanxi 030801, People's Republic of China

ABSTRACT: Fluoride is a widespread environmental pollutant that can induce low sperm quality and fertilizing ability; however, the underlying mechanism still remains unclear. Hence, we aimed to investigate the influence of fluoride on the sperm fertilizing ability via some key proteins in the epididymis. For this, 40 adult rats were assigned randomly into four groups. The control group was given distilled water, while the other three groups were given 25, 50, and 100 mg of NaF/L via drinking water for 56 days, respectively. After 1 day, epididymides were processed for sperm–egg binding, RNA extraction, western blot, and immunofluorescence analysis. Fluoride exposure reduced the ability of sperm to break down the egg cumulus cell layer. A further study revealed that fluoride altered the expression levels of genes and proteins related to acrosome reaction *in vivo*, including SPAM1, ACR, and PRSS21. However, fluoride only affected the expression of the ACR protein only in the epididymis but not in the testis. Fluoride also affected the expression levels of the membrane proteins CD9 and CD81 of epididymosomes in the epididymis. From the results, it can be concluded that fluoride exposure reduced the ability of sperm to break down the egg cumulus cell layer, which could be one of the reasons for decreased fertility ability in males treated with fluoride. These results provide some theoretical guidance and new ideas for treatments of low fertility, infertility, and other reproductive diseases.

KEYWORDS: fluoride, acrosome reaction, epididymis, sperm, rat, fertilizing ability

INTRODUCTION

Fluorine, an extremely reactive non-metallic element, exists in natural sources, including air, soil, water, food, coal, rock, and others, such as inorganic or organic compounds, and daily life environment widely in the form of diverse compounds.¹ Fluoride is one among a few chemicals that has been shown to cause effects in humans through drinking water;² nearly hundreds of millions of people in developing countries, such as China, India, and Bangladesh, are at risk of high fluoride toxicity.^{3,4} Besides drinking water, vegetables and fruits normally have 0.1–0.4 mg/kg of fluoride;² barley, rice, taro, yams, and cassava have been found to contain relatively high fluoride levels (e.g., about 2 mg/kg) and, thus, typically contribute to exposure. It is also reported that fluoride accumulates in the bones of canned fish, such as salmon and sardines. Fish protein concentrates may contain up to 370 mg/kg of fluoride.² Hence, the fluoride-induced toxicity has attracted worldwide attention. Many studies have shown that fluorine has adverse impacts on various tissue systems,^{5–8} including the reproductive system, and fertility.^{3,9} As a result of the overall fertility decline in industrialized countries, recent investigations have focused on the reproductive effects of fluoride. However, the mechanism underlying the fluoride-induced toxicity in the male reproductive system still remains unclear.

Mammalian spermatozoa undergo a series of complex structural and functional changes in the epididymis to mature and achieve fertilization capacity.⁹ The acrosome reaction,

which is one of the comprehensive evaluation indicators for sperm function, plays an essential role during the fertilization process.^{10,11} Fluoride has been shown to cause a wide variety of structural and functional defects in flagella and acrosomes.¹² Meanwhile, previous studies demonstrated that fluoride could induce alterations in the sperm fertilizing ability.¹³ However, most of the studies dealing with the reproductive system of fluoride focus on the morphological indices of sperm and spermatogenesis in testis;^{10–12} there are a few literature on sperm function as well as sperm maturation in the epididymis. The molecular mechanism of fluoride affecting sperm fertilization is still not fully clear.

Acrosin (ACR), serine protease PRSS21, and SPAM1 have been proven to play a vital role in sperm acrosomal response, sperm motility, and the fertilization process.^{14–20} SPAM1 protein produced by epididymal epithelial cells and transported by epididymosomes is also secreted by epididymal epithelial cells and installs into the sperm head.^{14,15} The epididymosomes represented by CD9, CD81, and MFGE8 are essential carriers for sperm maturation in the epididymis.^{21,22} The epididymosomes are responsible for the transport of sperm motility and fertilization ability.²³

Received: February 17, 2019

Revised: April 21, 2019

Accepted: April 22, 2019

Published: April 22, 2019

Table 1. Primer Sequences with Their Corresponding PCR Product Size

gene	sequence (5' → 3')	product size (bp)	GenBank accession number
<i>β-actin</i>	F: CTGGGTATGGAATCCTGTGG R: GCACTGTGTTGGCATAGAGG	97	NM_031144.3
<i>Spam1</i>	F: CTTTTGGAGGAGCTTTGCTG R: CCAGACCCAAACGAAAGTTG	133	NM_053967.2
<i>Acr</i>	F: AGCCGTCTTCAGTCCATACC R: GTAGACGCCGAGCAAAAGAC	138	X59254.1
<i>Prss21</i>	F: GTTGTGAGCTGGGGAATAGG R: CATCCCGTTTCGGATCATAG	108	NM_181477.2
<i>Mif</i>	F: CCGCACTTAACACCGTCCT R: CTGGGTGAGCTCGGAGAGAA	103	NM_031051.1
<i>Mfge8</i>	F: AGGAACAAGGAACCAGCAAG R: CACATAGCGAGCCATGAAAG	95	NM_001040186
<i>Atp2b4</i>	F: AGATCGCAGCCATCATATCC R: TCAATCCAGCCAGTTTCTCC	124	NM_001005871.1
<i>Dcxr</i>	F: GCAAGTTTGCTGAGGTGGAG R: GCAAAGCGGAACCAGTAGTC	87	NM_134387.1
<i>Cd9</i>	F: CGGTCAAAGGAGGTAGCAAG R: AGCCATAGTCCAATGGCAAG	100	NM_053018.1
<i>Cd81</i>	F: AGATCGCCAAGGATGTGAAG R: CAGTGTGGTCAGCGTATTGG	143	NM_013087.2
<i>Hsc70</i>	F: CCAAGCAGACCCAGACTTTC R: TGGCCCTTTCACCTTCATAC	81	NM_024351.2

Therefore, in this study, the fertilizing ability of sperm exposure to fluoride was evaluated first through *in vitro*. Second, the morphological structure of epididymal epithelial cells, the expressions of key proteins SPAM1, ACR, and PRSS21 related to acrosome reaction, and epididymosome functional genes, including CD9, CD81, and MFGE8, were investigated to elucidate the mechanism of fluoride-induced male reproductive toxicity and infertility.

MATERIALS AND METHODS

Animal Treatment. A total of 40 healthy adult male Sprague Dawley (SD) rats, weighting about 160–180 g, along with the standard diet were purchased from the Experimental Animal Center of Shanxi Medical University (Taiyuan, Shanxi, China) After acclimatization for 1 week, the animals were randomly divided into four groups, including the control group (drinking the distilled water) and three NaF-treated groups (drinking the distilled water containing 25, 50, and 100 mg/L NaF, respectively). All rats had free access to food and water under standard room temperature (RT, 22–25 °C), 12/12 h light/dark cycle, ventilation, and hygienic conditions. The drinking water intake was recorded to calculate the daily fluoride intake. After exposure for 8 weeks, all rats were sacrificed by cervical dislocation. The epididymides were removed, frozen quickly in liquid nitrogen, and stored at –80 °C for total RNA extraction and western blotting analysis. All animal experiments were performed in strict accordance with the regulations and guidelines of the Institutional Animal Care and Use Committee of Shanxi Agricultural University.

Sperm–Egg Binding. Four female SD rats (8 weeks old) were purchased from the Experimental Animal Center of Shanxi Medical University. A total of 25 units of pregnant mare serum gonadotropin (PMSG) and human chorionic gonadotropin (hCG), which were provided by Nanjing AIBI Biotech Co., Nanjing, Jiangsu, China, were given to each rat by intraperitoneal injection at an interval of 48 h. Metaphase-II-arrested eggs tightly packed with cumulus cells were collected from the oviductal ampulla 14 h after hCG injection and placed in a 200 μL tyramine hydrochloride solution (TYH medium, Nanjing AIBI Biotech Co., Nanjing, Jiangsu, China) covered with mineral oil; each TYH medium contains four to six eggs. The TYH medium was placed at 37 °C with 5% CO₂ incubator overnight prior to use.

The sperm–egg binding experiment was performed according to the study of Ohto et al.²⁴ The individual experiment in each group were repeated 5 times. Briefly, after sperm collection, sperm was rinsed into a plate with 1 mL of phosphate-buffered saline (PBS) in a Petri plate, and then PBS containing sperm was collected into a 1.5 mL EP tube, followed by centrifugation at 600g/min for 5 min. A total of 20 μL of sperm was taken into the bottom of the tube containing 380 μL of TYH medium with Hoechst 33342 (2.5 μg/mL, Solarbio Science & Technology Co., Beijing, China) and incubated for 10 min at 37 °C with 5% CO₂. Then, 20 μL of sperm was taken from 400 μL of TYH medium into 100 μL of TYH medium, followed by incubation for 50 min at 37 °C with 5% CO₂. A total of 20 μL of sperm was taken from 120 μL of TYH medium into 200 μL of TYH medium with the eggs and then incubated for 2 h at 37 °C under 5% CO₂. Finally, the eggs and sperm were fixed by 8% paraformaldehyde (PFA) for 15 min. Then, images were taken immediately under a fluorescence microscope (DMI3000 B, LEICA, Oskar-Barnack-Straße, Germany).

Quantitative Real-Time Polymerase Chain Reaction (PCR). Total RNAs were extracted from cauda epididymides and testis with TRIZOL reagent (Takara, Dalian, Liaoning, China). The concentration and quality of total RNA were analyzed by a NanoDrop 2000 spectrophotometer (Thermo Fisher, Wilmington, DE, U.S.A.). RNA was reverse-transcribed using a PrimeScript Reverse Transcription (RT) Master Mix kit. Quantitative real-time PCR was performed using the QuantStudio 7 Flex quantitative real-time PCR system (Life Technologies, Carlsbad, CA, U.S.A.) and SYBR Premix Ex Taq II kit. The primers were designed with Primer3Plus online (<http://www.primer3plus.de/cgi-bin/dev/primer3plus.cgi>) and biosynthesized by Sangon Biotech Co., Ltd. (Shanghai, China) according to the complete cDNA sequences deposited in GenBank (Table 1). The amplification conditions were maintained as follows: after initial denaturation at 95 °C for 120 s, 40 PCR cycles were started with thermocycling conditions at 95 °C for 15 s, 60 °C for 30 s, and 72 °C for 6 s. Each sample was measured in duplicate. Data were analyzed using the 2^{–ΔΔC_T} method.

Western Blotting Analysis. The cauda epididymis tissue samples (50 mg of tissue; *n* = 6/group) were homogenized in radio-immunoprecipitation assay (RIPA) buffer (KeyGEN Biotech, Nanjing, Jiangsu, China) with 1% phenylmethylsulfonyl fluoride (PMSF, Beyotime Biotechnology, Shanghai, China). The homogenate

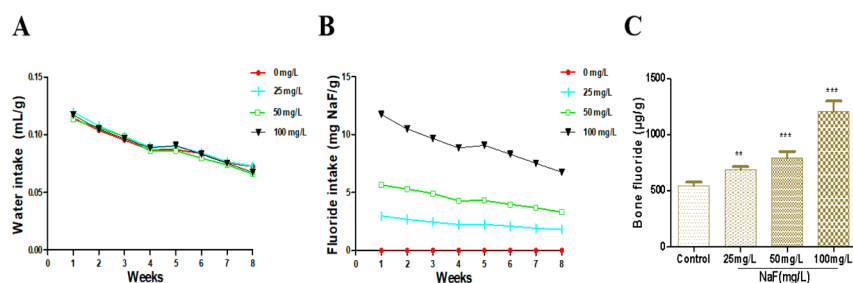


Figure 1. Water intake and bone fluorine levels in rats. (A) Water intake per gram of body weight of rats in all groups. (B) Fluoride intake per gram of body weight of rats in all groups. (C) Fluoride contents in the femur of rats in all groups. The values are presented as the mean \pm SEM ($n = 6$). (***) $p < 0.001$ and (**) $p < 0.01$ indicate significant differences compared to the control.

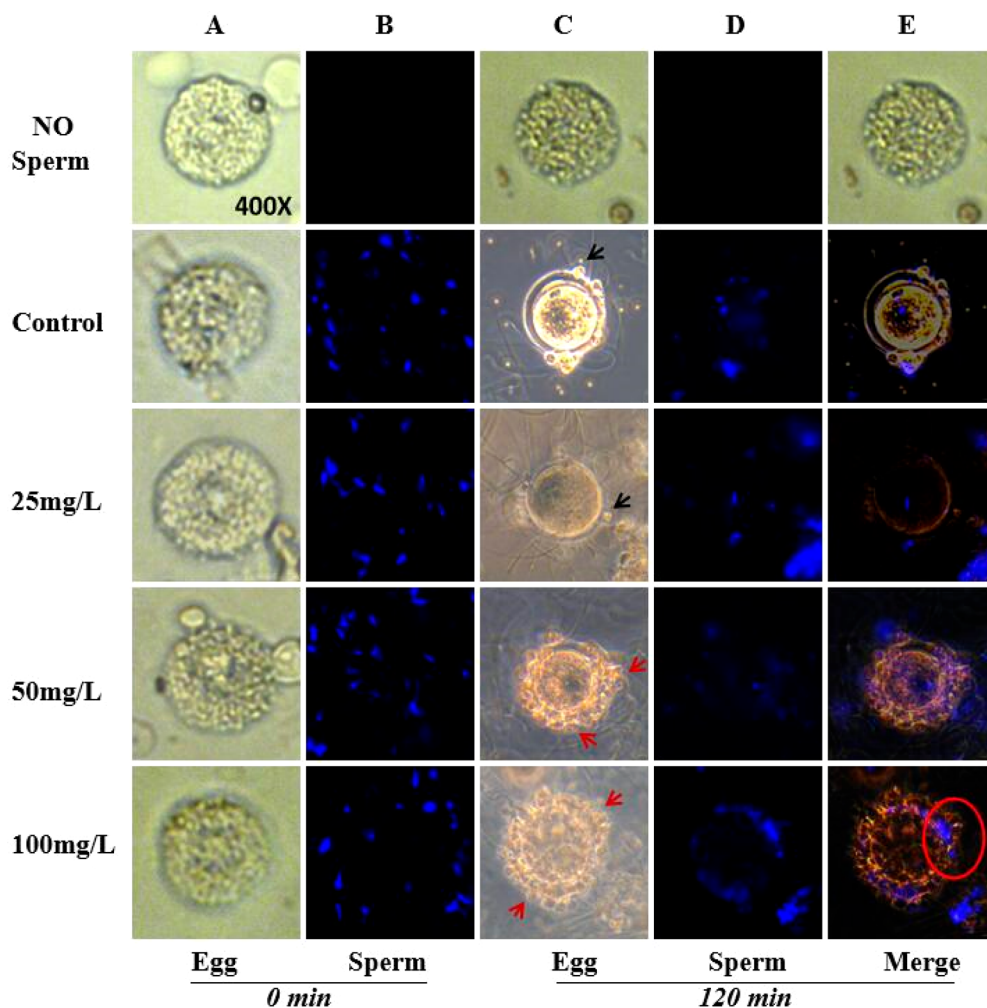


Figure 2. Effects of fluorine on the function of sperm to break down the cumulus cell layer. (A) Images from normal mature eggs prepared for fertilization. (B) Images of spermatozoa stained with Hoechst 33324 (blue) obtained from rats treated with 0, 25, 50, and 100 mg/L NaF for 8 weeks. The first line is the blank control without spermatozoa. (C) Representative images of eggs after sperm–egg binding for 120 min. The black arrows represent a small number of granulosa cells on the surface of the egg. The red arrows indicate that the cumulus cell layers have not been dispersed and a large number of granulosa cells gather together on the surface of the eggs. (D) Morphological images of sperm after sperm–egg binding for 120 min. The first line is the group without sperm. (E) Merged images from panels C and D. The red circle shows the sperm that are blocked by the radiation crown.

solutions were incubated on ice for 40 min and then centrifuged at 12000g for 10 min at 4 °C. Supernatants were used for western blotting analysis. Protein concentrations of the epididymis tissue samples were determined by the bicinchoninic acid (BCA) protein assay kit (KeyGEN Biotech, Nanjing, Jiangsu, China), at 562 nm wavelength. A total of 60 μ g of total protein per sample was loaded on 12% sodium dodecyl sulfate (SDS) polyacrylamide electrophoresis gels, and then proteins were transferred to nitrocellulose (NC)

membranes. The NC membranes were blocked with 5% (w/v) non-fat dry milk in Tris-buffered saline (TBS) containing 0.05% Tween 20 for 2 h at RT and then incubated with the primary antibodies against SPAM1 (1:1000 dilution), ACR (1:1000 dilution), PRSS21 (1:1000 dilution), CD9 (1:500 dilution), CD81 (1:500 dilution), and β -actin (1:1000 dilution) overnight at 4 °C. Primary antibodies were used as follows: mouse anti- β -actin monoclonal antibody (60008-1-Ig) was purchased from Proteintech Group (Wuhan, Hubei, China); rabbit

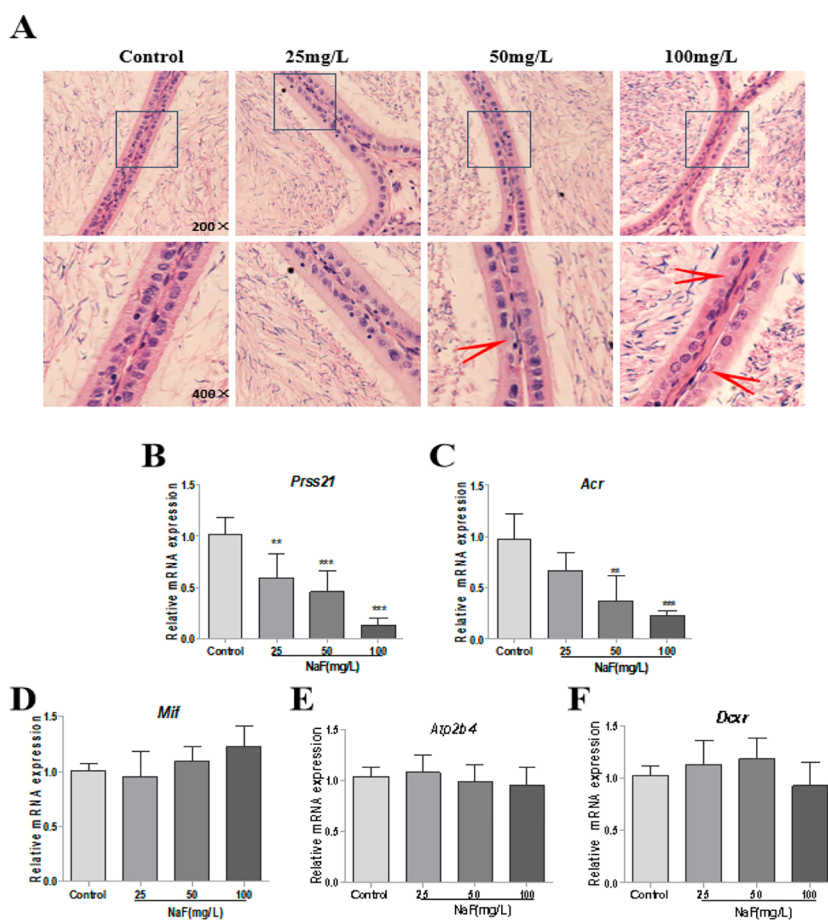


Figure 3. Effects of fluoride on morphology of caudal epididymides and expressions of acrosome-reaction-related proteins. (A) Cauda epididymal luminal epithelial cells were detected by hematoxylin and eosin (HE) stain. The second line of pictures is an enlarged version of the black square in the first line. Red arrows marked the missing nuclei. (B, C, D, E, and F) Levels of *Acr*, *Prss21*, *Mif*, *Atp2b4*, and *Dcxr* mRNA expression, respectively, were detected by real-time PCR. β -actin was used as a control. The values are presented as the mean \pm SEM ($n = 5$). (***) $p < 0.001$, (**) $p < 0.01$, and (*) $p < 0.05$ indicate significant differences compared to the control.

anti-PRSS21 polyclonal antibody (A16100), rabbit anti-SPAM1 polyclonal antibody (A2120), and rabbit anti-CD9 monoclonal antibody (A10789) were purchased from AB clonal (Wuhan, Hubei, China); rabbit anti-ACR antibody (bs-5151R) was purchased from Bioss (Beijing, China); and rabbit anti-CD81 antibody (DF-2306) was purchased from Affinity (Changzhou, Jiangsu, China). The membranes were washed 3 times with phosphate-buffered saline containing Tween 20 (PBST) for 5 min each, followed by incubation with fluorescein isothiocyanate (FITC)-conjugated secondary antibody (Proteintech Group, Wuhan, Hubei, China) at RT for 2 h. Protein bands on membranes were detected by enhanced chemiluminescence (ECL, Beyotime Biotechnology, Shanghai, China). A FluorChem Q Imaging System and its analysis software system (ProteinSimple, San Jose, CA, U.S.A.) were used to acquire, quantify, and analyze the intensity of the protein bands.

Immunofluorescence. Epididymis tissue samples were fixed in 4% PFA for 24 h, washed in a vessel with tap water for 10 h, and dehydrated in a series of graded ethanol. Samples were subsequently embedded in paraffin and sectioned at 5 μ m thickness onto slides. Sections were washed with a decreasing series of ethanol (from 100 to 50%) and rinsed with distilled water for 5 min. Sections were boiled for 15 min in sodium citrate buffer for antigen retrieval, rinsed in PBS, and blocked with 5% bovine serum albumin (BSA) for 1 h at RT; Sperm was collected from the cauda epididymal of male rats in all groups, centrifuged at 600g/min for 5 min, and washed twice with 10 mL of PBS. After that, 20 μ L of sperm was taken in the bottom of the tube into 1 mL of PBS; 10 μ L of sperm was taken from PBS for smears; and then smears were incubated in 100% methanol for 30 min

to fix the dried sperm. Afterward, the sections were blocked with 5% BSA for 1 h at RT.

All sections and sperm smears were incubated with the primary antibodies overnight at 4 $^{\circ}$ C. After rinsed 3 times with PBST (1 \times , pH 7.5), the sections and sperm smears were incubated with FITC-conjugated secondary antibody (Proteintech Group, Wuhan, Hubei, China) for 1 h at RT and then rinsed 3 times with PBST. Finally, the sections and sperm smears were sealed with a sealant containing 4',6'-diamidino-2-phenylindole (DAPI, Solarbio Science & Technology Co., Beijing, China), and images were taken immediately under a fluorescence microscope (BX53F, Olympus, Japan).

Statistical Analysis. GraphPad Prism7 software was employed to statistical analysis. Each data was expressed as the mean \pm standard error of mean (SEM) of at least three independent experiments. Statistical differences were determined using one-way analysis of variance (ANOVA), and differences were considered statistically significant with a p value of <0.05 .

RESULTS

Fluoride Intake and Bone Fluoride Levels in Rats.

During the 8 week exposure period, the weekly drinking water intakes and fluoride intakes were calculated in rats of all groups once and the data were shown graphically in Figure 1. From the results, the water consumptions did not significantly change among four groups, and the fluorine intake [mg of NaF/body weight (BW)] levels via drinking water were increased in a dose-dependent manner in three NaF-treated

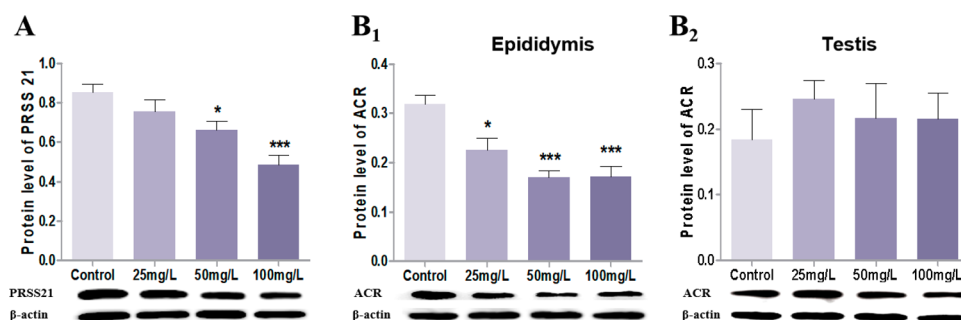


Figure 4. Effects of fluoride on PRSS21 and ACR expression in the epididymis and testes. (A) Changes in expression levels of PRSS21 in caudal epididymides induced by fluoride detected by western blot. (B₁ and B₂) Levels of protein expression of ACR in caudal epididymides and testis of rats treated with 0, 25, 50, and 100 mg/L NaF, respectively. β -actin was used as a control. The values are presented as the mean \pm SEM ($n = 4$). (***) $p < 0.001$ and (*) $p < 0.05$ indicate significant differences compared to the control.

groups compared to the controls. Meanwhile, after 8 weeks of exposure, the femur fluorine contents were elevated significantly in NaF groups in a dose-dependent manner. From the results, it was obvious that the fluoride exposure model was established successfully.

Fluoride Interferes with the Fertilizing Ability of Sperm. The fertilizing ability of sperm exposed to fluoride was evaluated by the sperm–egg bind experiment. The morphology of egg and sperm at the beginning and end of the sperm–egg binding reaction was shown in Figure 2. The cumulus cell layer of the egg was almost completely decomposed in control groups; only a small amount of undetached granulosa cells adhered to the surface of the egg; and the matrix between the granulosa cells has been broken down (Figure 2C). Similarly, the same situation was also observed in the 25 mg/L NaF-treated group. However, the cumulus cell layer of the egg was not completely decomposed in 50 and 100 mg/L NaF-treated groups (red arrowa in Figure 2C). A large number of granulosa cells were observed to be clustered together, and the matrix of these cells was not broken down in 50 and 100 mg/L NaF-treated groups. The large number of unseparated granulosa cells still adhered to the surface of the egg (circle in Figure 2E), blocking the sperm to move forward, and hence, the sperm (blue) was observed outside the radiation crown. These findings indicate that fluoride reduces the ability of sperm to break down the cumulus cell layer, which decreased the fertilizing capability of sperm.

Changes in the Morphology of the Epididymis and Expressions of Acrosome-Reaction-Related Proteins Induced by Fluoride. The closely packed nuclei in epithelial cells of epididymis tissues were detected in the control and NaF-treated groups. The results showed that the some of the nuclei were found to be missing in the epithelial cells that occurred in the 50 and 100 mg/L NaF-treated groups (red arrows in Figure 3A). The mRNA expression levels of acrosome-reaction-related genes, such as *Acr*, *Prss21*, *Mif*, *Atp2b4*, and *Dcxr*, were examined by real-time PCR. The results demonstrated that mRNA expression levels of *Prss21* in epididymides of rat exposed to 50 and 100 mg/L NaF-treated groups decreased significantly compared to the controls ($p < 0.01$ and $p < 0.001$; Figure 3B). Meanwhile, the significant decreases in the levels of *Acr* mRNA expression were noted in the 25, 50, and 100 mg/L NaF-treated groups ($p < 0.01$ and $p < 0.001$; Figure 3C). Nevertheless, no significant changes were observed in *Mif*, *Atp2b4*, and *Dcxr* mRNA expression levels in the epididymis of rats administrated to fluoride (panels D–F of Figure 3).

Subsequently, protein expression levels of PRSS21 and ACR in caudal epididymides were validated by western blot. The results revealed a significant decrease in PRSS21 expression levels in epididymides of all NaF-treated groups; however, ACR expression was decreased significantly in epididymides of rats exposed to 50 and 100 mg/L NaF groups ($p < 0.05$ and $p < 0.001$) only compared to the control group (panels A and B₁ of Figure 4). With the results of ACR expression in both epididymides and testicular tissues, the levels of ACR expression in testis were determined further. The result demonstrated that fluoride exposure did not alter the levels of ACR protein in testis of rat (Figure 4B₂). These results suggest that fluoride exposure downregulated the transcripts and protein expression of sperm acrosome response functional proteins ACR and PRSS21, which further resulted in alteration in the structural morphology of the epididymis and decreased fertility.

Fluoride Reduces SPAM1 Protein Expression in Epididymosomes and Spermatozoon. SPAM1, transcribed in testis and translated in epididymides, plays a key role during sperm acrosome reaction and maturation. Therefore, the mRNA expression levels of *Spam1* in testis and SPAM1 expression in epididymides tissues were examined by real-time PCR, immunofluorescence, and western blot, respectively. The results showed that both *Spam1* mRNA expression in testes and protein levels in epididymides were decreased significantly in 50 and 100 mg/L NaF-treated groups compared to the control group (panels A and B of Figure 5). The immunofluorescence analysis showed that SPAM1 expression was located in the epithelial tissues of caudal epididymides (white arrows in Figure 5C), which is consistent with the luminal epithelial-secreting cells (red triangle). The fluorescence intensity of SPAM1 in epididymides tissues of 50 and 100 mg/L NaF-treated groups reduced significantly compared to the controls (Figure 5E). Meanwhile, the expressions of SPAM1 were observed in spermatozoon of caudal epididymides of the control and three fluoride-treated groups (Figure 5D). On the basis of the fluorescence intensity levels, the expression levels of SPAM1 in spermatozoon of the caudal epididymides were found to be decreased significantly in both 50 and 100 mg/L NaF-treated groups compared to the control group (Figure 5F). These results suggest that fluoride exposure downregulated the SPAM1 expression in both epididymosomes and spermatozoon of epididymides, which interfered with sperm acrosome reaction and maturation.

Expressions of Epididymosome Functional Proteins Induced by Fluoride. Epididymosomes, located in the

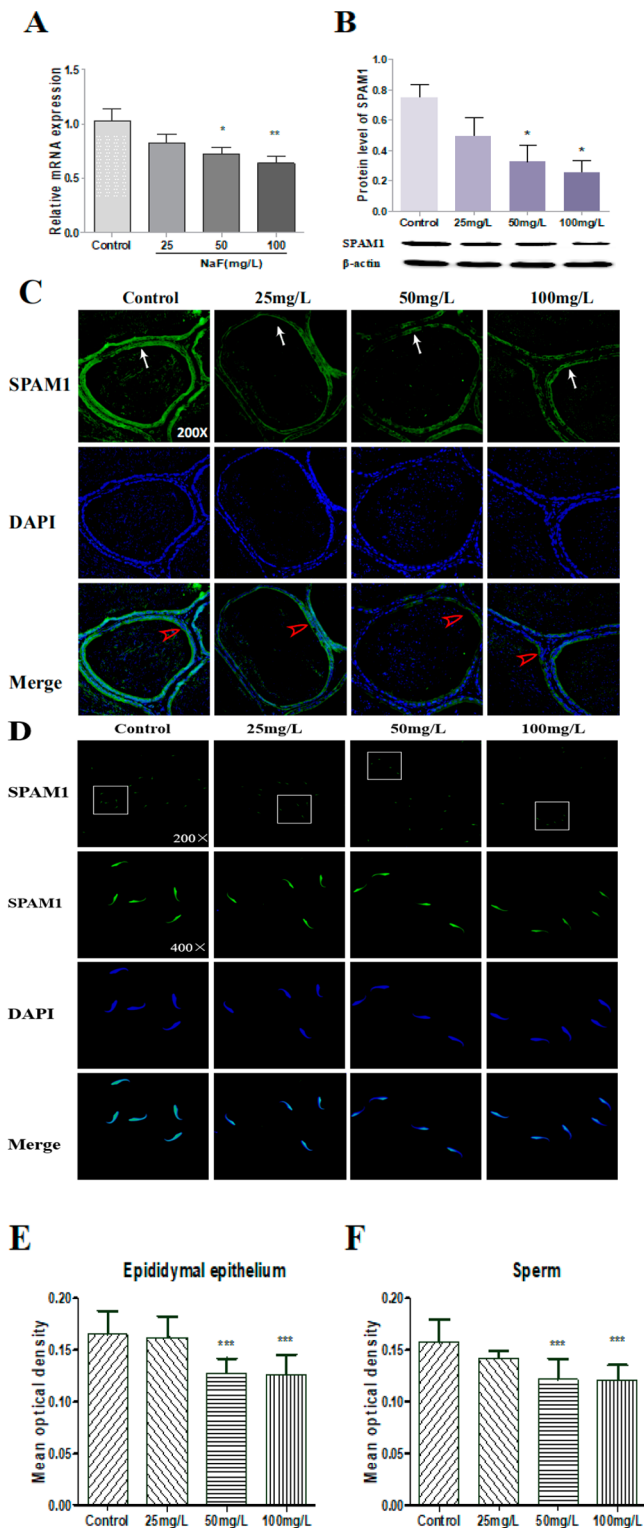


Figure 5. Effects of fluoride on SPAM1 expression in testis, cauda epididymis, and sperm. (A) mRNA expression of *Spami* in testis detected by real-time PCR. (B) Expression levels of SPAM1 in cauda epididymides detected by western blot. β -actin was used as a control. The data are presented as the mean \pm SEM ($n = 5$). (***) $p < 0.001$ and (*) $p < 0.05$ indicate significant differences compared to the control. (C and D) Representative images of SPAM1 expression in the epididymal luminal epithelial and spermatozoa in cauda epididymis of rats exposed to 0, 25, 50, and 100 mg/L NaF, respectively. The white arrows indicate the epididymal luminal epithelial, and the red triangles show the epithelial cells of the

Figure 5. continued

epididymis. The green color fluorescence is SPAM1 positive cells, and cell nuclei were stained with DAPI (blue). The white square shows the fields of original magnification (200 \times). (E) Analysis results of average optical density of SPAM1 expression in the epithelium of the cauda epididymides. (F) Analysis results of average optical density of SPAM1 expression in spermatozoa of sperm. The data are presented as the mean \pm SEM ($n = 6$). (***) $p < 0.001$ indicates significant differences compared to the control.

luminal fluid of the epididymis, are secreted by epididymal epithelial cells and play a vital role in sperm maturation. Hence, the mRNA expression levels of the functional proteins *Cd9*, *Cd81*, *Mfge8*, and *Hsc70* in epididymosomes were examined by real-time PCR. The results showed that the levels of *Cd9* mRNA expression decreased in epididymides of rats exposed to 25, 50, and 100 mg/L NaF ($p < 0.01$ and $p < 0.001$; Figure 6A). Meanwhile, a significant increase in *Cd81*

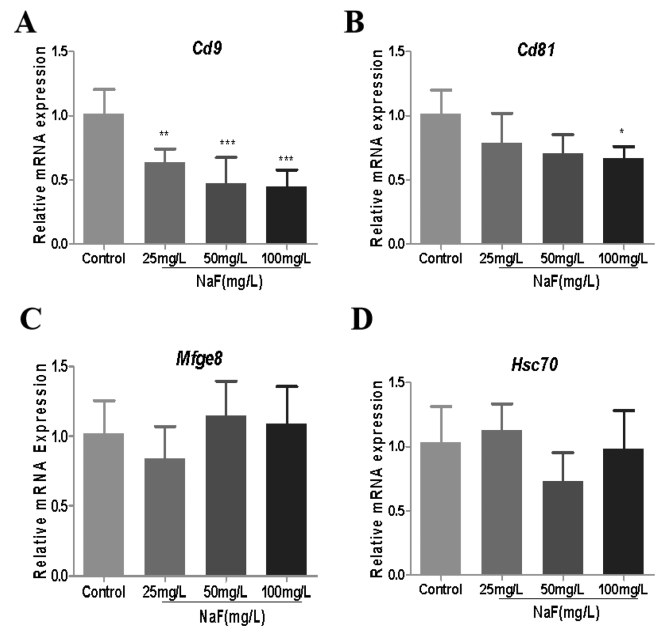


Figure 6. Effects of fluoride on the expression of functional genes of epididymosomes in cauda epididymis. (A–D) mRNA expression levels of *Cd9*, *Cd81*, *Mfge8*, and *Hsc70* in epididymides of rat exposure to the different concentrations of 0, 25, 50, and 100 mg/L NaF detected by real-time PCR. β -actin was used as the control. The values are presented as the mean \pm SEM ($n = 5$). (***) $p < 0.001$, (**) $p < 0.01$, and (*) $p < 0.05$ indicate significant differences compared to the control.

mRNA expression was observed in epididymides from the 100 mg/L NaF-treated group compared with the control group ($p < 0.05$; Figure 6B). However, no significant changes were observed in mRNA expression levels of *Mfge8* and *Hsc70* (panels C and D of Figure 6).

Subsequently, CD9 and CD81 expression in caudal epididymides was evaluated by western blot. The results showed that a significant decrease in CD9 expressions of epididymides was observed in 50 and 100 mg/L NaF-treated groups. However, CD81 expression decreased significantly only in the rats exposed to the 100 mg/L NaF group ($p < 0.01$, $p < 0.05$, and $p < 0.001$) compared to the control group (panels A and B of Figure 7). Furthermore, the immuno-

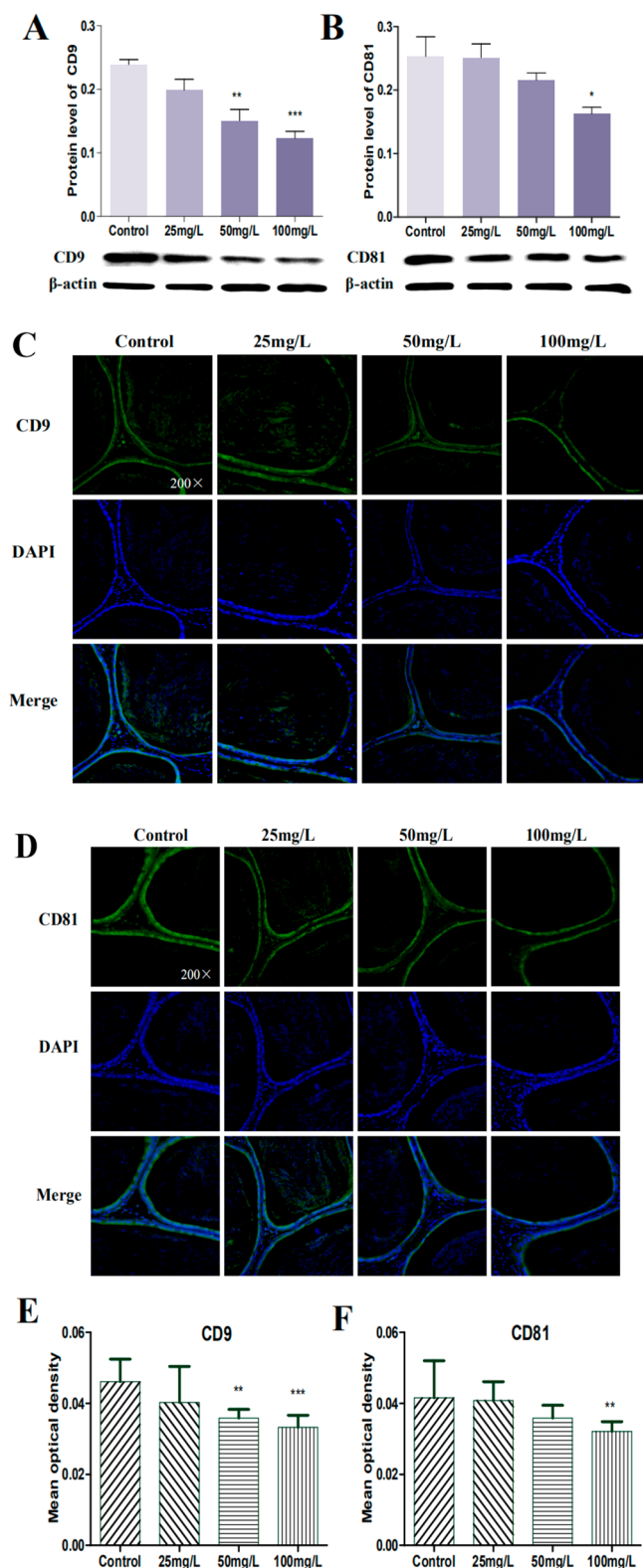


Figure 7. Effects of fluoride on CD9 and CD81 expression in caudal epididymides. (A and B) Changes in CD9 and CD81 expression in caudal epididymides of rats treated with 0, 25, 50, and 100 mg/L NaF by western blot. β -actin was used as the control. The values are presented as the mean \pm SEM. (*) $p < 0.05$, (**) $p < 0.001$, and (***) $p < 0.001$ indicate significant differences compared to the control. (C and D) Representative images of CD9 and CD81 expression localizations in cauda epididymides of rats by immunofluorescence, respectively. The green color fluorescence is CD9 and

Figure 7. continued

CD81 positive cells, and cell nuclei were stained with DAPI (blue). (E and F) Analysis results of average optical density of CD9 and CD81 expression in the caudal epididymides of rats. The data are presented as the mean \pm SEM. (**) $p < 0.001$ and (***) $p < 0.001$ indicate significant differences compared to the control.

fluorescence analysis showed that CD9 and CD81 expression was located in the epithelial tissues and the epididymal lumen of caudal epididymides (panels C and D of Figure 7). The fluorescence intensity of CD9 in epididymides tissues from 50 and 100 mg/L NaF-treated groups reduced significantly, and the fluorescence intensity of CD81 in epididymides tissues of 100 mg/L NaF-treated groups reduced significantly compared to their respective control groups (Figure 7F). This suggests that altered levels of CD9 and CD81 induced by fluoride may be responsible for the decreased fertilizing ability of sperm.

DISCUSSION

In general people tend to be exposed to high levels of fluoride through drinking water, food, and air, although the U.S. Health and Human Services Department recommended 0.7–1.2 mg of fluoride/L of water as the safe range in 2015.² Even fluoride ion concentrations in groundwater have been reported to be as high as 48 mg/L.³ Hence, in the present study, rats were maximally treated with 100 mg/L NaF, corresponding to 45.2 mg/L fluoride ion, which is considered as the risk of actual fluoride exposure on a human. The results from the fluoride levels in drinking water and femur indicate that the fluoride exposure model is successful.

Mammalian fertilization is a complex cascade process consisting of sperm migration through the female reproductive tract, physiological changes to sperm, such as sperm capacitation and acrosome reaction, and sperm–egg interaction in the oviduct *in vivo*.²⁵ It is well-known that sperm has a very significant genetic function and profound effect on fertility, embryos, and heredity.⁹ Previous studies demonstrated that fluoride induced alterations in multiple functions of sperm during fertilization, including morphology,¹³ capacitation,¹³ hyperactivation,²⁶ and chemotaxis.²⁷ Furthermore, the spermatogenesis, sperm concentration, sperm survival, sperm motility, and overall fertility decreases were affected by fluoride administration in rodents.^{2,10,13} After 4 weeks of 100 mg/L NaF exposure in male mice, the pregnancy rate of untreated female mice is reduced by 10%; however, it was increased to 50% after 10 weeks.²⁸ An *in vitro* fertilization experiment showed that the spermatozoa fertilization ability of fluoride-exposed rats was significantly reduced ($13 \pm 5.10\%$) in comparison to the control group ($72 \pm 4.69\%$).²⁹ Our previous studies also observed that the pregnancy rate of females was decreased by 36.5%, and the litter rate also decreased significantly when the healthy females mated with the male mice treated with 150 mg/L NaF for 105 days (unpublished data). Hence, in the present study, we aimed to assess whether fluoride exposure effects sperm fertilization via altering with the acrosome reaction of spermatozoa and key protein expressions in the epididymis.

The acrosome reaction is a series of changes in the sperm acrosome before fertilization. In this process, the sperm needed to erode the cumulus cell layer and the zona pellucida (ZP), opening a channel to access the egg.¹¹ Kim et al. reported that the rate of capacitation and the acrosome reaction were altered

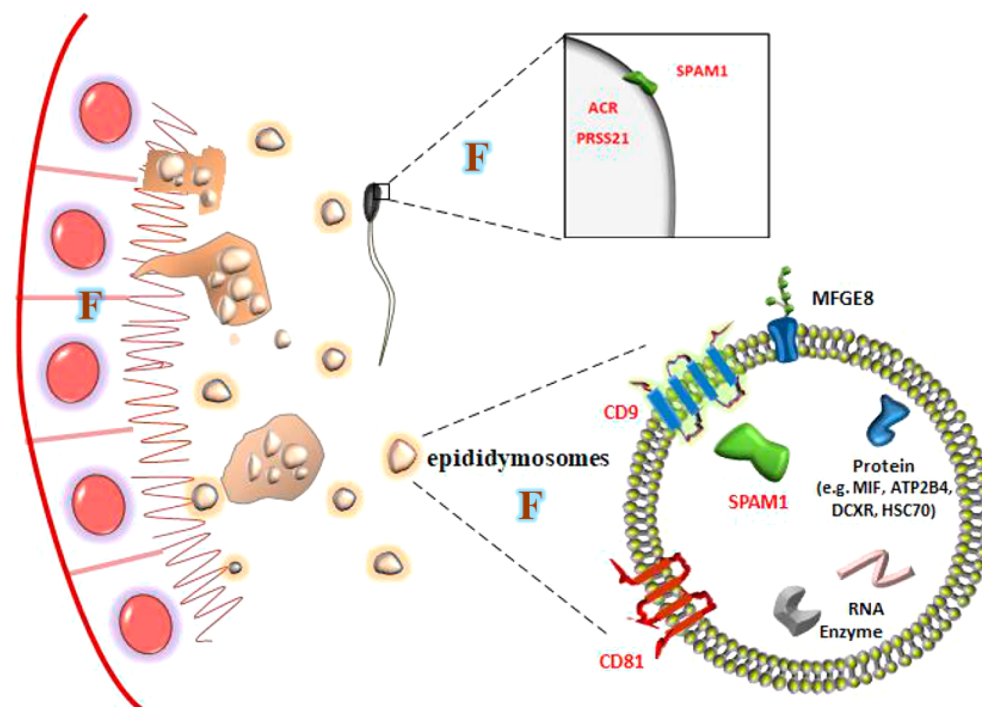


Figure 8. Schematic diagram of fluoride interfering with the sperm fertilizing ability. Proteins highlighted in red color decreased significantly by fluoride. PRSS21 and ACR expression in sperm and SPAM1 protein were produced by epididymal epithelial cells and transported by epididymosomes, which install into the sperm head in the rat epididymis. Epididymosomes are secreted by epididymal epithelial cells and present in the luminal fluid of the epididymis. CD81, CD9, and MFGE8 are located on the membrane of epididymosomes, and HSC70, MIF, ATP2B4, and DCXR exist in the inside of the epididymosomes.

when mouse spermatozoa were incubated with a range of concentrations of 2.5, 5, and 10 mM NaF.³⁰ Another experiment of combining sperm and the egg without cumulus cells reported that fluoride maybe interfered with the segmental processes of the acrosome reaction.²⁹ As we know, the acrosome reaction *in vivo* is essential for sperm to break down this layer of cells and then reach ZP.¹⁴ Therefore, in the present study, the binding experiment with sperm *in vivo* models and intact eggs was conducted to assess the true acrosome reaction status caused by fluoride. The result provides new evidence that fluoride exposure reduced the ability of sperm to break down the egg cumulus cell layer.

The epididymis was an important reproductive organ that is responsible for transmission, concentration, and storage of sperm in male mammals.^{31,32} Spermatozoa attain fertilization ability after undergoing a series of structural and functional alterations in the epididymis.^{31,33,34} Therefore, we first observed the morphological features of the epididymal luminal epithelial cells after fluoride exposure. The results of the current study revealed that fluoride exposure led to the loss of nuclei in epithelial cells. This phenomenon indicates that fluorine may impair the ability of sperm to break down the cumulus cell layer by affecting the secretion of multiple key proteins in the epididymis.

Sperm serine protease and proteasome have long been believed to play an important role in the fertilization process.^{15–20} ACR was the trypsin-like serine protease in the sperm acrosome.¹⁸ An *in vitro* fertilization study revealed that the ACR-disrupted sperm spread more slowly to cumulus cells than wild-type sperm.¹⁹ The serine protease PRSS21, also known as testosterone, directs epididymal sperm cell maturation and sperm fertilization.²⁰ PRSS21-deficient sper-

matozoa show decreased motility and angulated and fragile necks.²⁰ The sperm in double-knockout ACR/PRSS21 mice were defective in penetration through the cumulus matrix to reach ZP.¹⁶ The present study further confirmed that fluoride exposure downregulated the expressions of ACR and PRSS21 in mature sperm acrosome of the cauda epididymis. On account of the importance of ACR in the spermatogenesis stage of testis,¹⁷ we also evaluated the expression levels of ACR in testis of rat exposed to fluoride. From the results, we found that fluoride only affects the expression of ACR protein in the epididymis but not in the testis. In addition, MIF, ATP2B4/PMCA4, and DCXR/P34H are important to sperm motility and fertilization. For instance, MIF was involved in sperm motility and was associated with sperm fiber density.^{35,36} ATP2B4 mainly regulates the vitality of sperm.^{37,38} DCXR increases the rate penetration of sperm into the cumulus cell layer.³⁹ However, in the present study, fluoride did not affect the expression of *Mif*, *Atp2b4*, and *Dcxr* protein mRNA levels in the whole cauda epididymis.

It is well-known that sperm protein SPAM1/PH20 is closely related to the ability of sperm to break down the cumulus cell layer.^{14,15,40} Fertilization in mammals requires the sperm to pass through the layer consisting of the extracellular matrix of cumulus cells and reach the ZP in eggs. The egg cumulus cell layer was abundant in hyaluronic acid.⁴⁰ Hyaluronic acid was a major component of the extracellular matrix, and it was hydrolyzed by hyaluronidase into oligosaccharides.⁴¹ SPAM1 was glycosylphosphatidylinositol anchored only on the plasma membrane of sperm and has hyaluronidase activity.¹⁵ When the enzyme activity of SPAM1 was blocked, sperm were incapable of entering into the cumulus cell layer.¹⁴ The loss of SPAM1 activity resulted in a remarkable increased accumu-

lation of sperm on the surface or outer edge of the cumulus cell layer.⁴² In the present study, SPAM1 expression in whole cauda epididymis was decreased significantly by NaF. On the basis of the results of SPAM1 expression levels in both epididymal epithelium and sperm of cauda epididymis,⁴³ we further examined the expression of SPAM1 protein in the epididymal luminal epithelial cells and sperm by immunofluorescence. The results showed that expression of SPAM1 protein in epididymal luminal epithelial cells was significantly affected by fluoride, which seems to be explained by the phenomenon of the missing nuclei in epididymal luminal epithelial cells (Figure 3A); after all, SPAM1 protein was secreted by epididymal luminal epithelial cells.⁴⁴ Interestingly, the expression of SPAM1 protein in sperm was also reduced by NaF, indicating that the process of transferring SPAM1 to the sperm head may be affected by fluoride.

As we all know, the epididymosomes, which are an exosome and secreted by epididymal epithelial cells in the epididymis, play a crucial role in the transfer of SPAM1 protein from the epididymal luminal to the sperm head.²³ The epididymosomes promote sperm maturation mainly by transporting proteins and RNA required for sperm maturation and fertilization.²³ The formation of epididymosomes includes the following steps: (1) secretion of apical vesicles by epithelial cells, (2) release of vesicles into the lumen of the epididymis, and (3) release of epididymosomes by vesicle rupture.⁴⁵ CD9 and CD81 were transmembrane junction proteins on the membrane of epididymosomes, which can promote inter- and intracellular signal transduction.²¹ MFGE8 was also a membrane protein, whose domain C2 can bind to phosphatidylserine residues exposed on the surface of sperm cells.²² In our study, fluoride affected the expression of the membrane proteins CD9 and CD81 in the whole cauda epididymis. These results suggest that the changes in the key protein SPAM1 expression in sperm by fluoride may be evaluated via affecting the epididymosomes (Figure 8).

As stated above, our current study provides the evidence that fluoride affects the ability of sperm to break down the cumulus cell layer of the egg. Moreover, the effects of fluoride on the expressions of acrosomal reaction key proteins SPAM1, ACR, and PRSS21 and membrane proteins CD9 and CD81 were evaluated, and these results contribute to the elucidation of the underlying mechanisms of fluoride-induced male reproductive toxicity.

AUTHOR INFORMATION

Corresponding Author

*Telephone/Fax: +86-354-6288335. E-mail: jianhaiz@163.com and/or jianhaiz@sxau.edu.cn.

ORCID

Jianhai Zhang: [0000-0001-6005-8376](https://orcid.org/0000-0001-6005-8376)

Funding

This research was supported by the National Natural Science Foundation of China (Grants 31741120 and 31172380) and a research project supported by the Shanxi Scholarship Council of China (2017-70).

Notes

The authors declare no competing financial interest.

REFERENCES

- (1) Sun, Z. L.; Li, S. J.; Yu, Y. X.; Chen, H. Y.; Ommati, M. M.; Manthari, R. K.; Niu, R. Y.; Wang, J. D. Alterations in epididymal proteomics and antioxidant activity of mice exposed to fluoride. *Arch. Toxicol.* **2018**, *92*, 169–180.
- (2) *Fluoride in Drinking-Water*; Fawell, J., Bailey, K., Chilton, J., Dahi, E., Fewtrell, L., Magara, Y., Eds.; World Health Organization (WHO): Geneva, Switzerland, 2006.
- (3) Zhang, J. H.; Zhu, Y. C.; Shi, Y.; Han, Y. L.; Liang, C.; Feng, Z. Y.; Zheng, H. P.; Eng, M.; Wang, J. D. Fluoride-Induced Autophagy via the Regulation of Phosphorylation of Mammalian Targets of Rapamycin in Mice Leydig Cells. *J. Agric. Food Chem.* **2017**, *65*, 8966–8976.
- (4) Mikkonen, H. G.; Dasika, R.; Drake, J. A.; Wallis, C. J.; Clarke, B. O.; Reichman, S. M. Evaluation of environmental and anthropogenic influences on ambient background metal and metalloid concentrations in soil. *Sci. Total Environ.* **2018**, *624*, 599–610.
- (5) Gao, Y.; Liang, C.; Zhang, J. H.; Ma, J. J.; Wang, J. M.; Niu, R. Y.; Tikka, C. J.; Wang, Y. W.; Wang, J. D. Combination of Fluoride and SO₂ induce DNA damage and morphological alterations in male rat kidney. *Cell. Physiol. Biochem.* **2018**, *50*, 734–744.
- (6) Zhou, B. H.; Zhao, J.; Liu, J.; Zhang, J. L.; Li, J.; Wang, H. W. Fluoride-induced oxidative stress is involved in the morphological damage and dysfunction of liver in female mice. *Chemosphere* **2015**, *139*, 504–511.
- (7) Niu, R. Y.; Chen, H. j.; Manthari, R. K.; Sun, Z. L.; Wang, J. M.; Zhang, J. H.; Wang, J. D. Effects of fluoride on synapse morphology and myelin damage in mouse hippocampus. *Chemosphere* **2018**, *194*, 628–633.
- (8) Oliva, R.; de Mateo, S.; Estanyol, J. M. Sperm cell proteomics. *Proteomics* **2009**, *9* (4), 1004–1017.
- (9) Ge, Y. M.; Niu, R. Y.; Zhang, J. H.; Wang, J. D. Proteomic analysis of brain proteins of rats exposed to high fluoride and low iodine. *Arch. Toxicol.* **2011**, *85* (1), 27–33.
- (10) Zakrzewska, H.; Udala, J.; Blaszczyk, B. In vitro influence of sodium fluoride on ram semen quality and enzyme activities. *Fluoride* **2002**, *35* (3), 153–160.
- (11) Hirohashi, N.; Yanagimachi, R. Sperm acrosome reaction: Its site and role in fertilization. *Biol. Reprod.* **2018**, *99* (1), 127–133.
- (12) Sun, Z. L.; Wei, R. F.; Luo, G. Y.; Niu, R. Y.; Wang, J. D. Proteomic identification of sperm from mice exposed to sodium fluoride. *Chemosphere* **2018**, *207*, 676–681.
- (13) Long, H.; Jin, Y.; Lin, M.; Sun, Y.; Zhang, L. A. Fluoride toxicity in the male reproductive system. *Fluoride* **2009**, *42* (4), 260–276.
- (14) Lin, Y.; Mahan, K.; Lathrop, W. F.; Myles, D. G.; Primakoff, P. A hyaluronidase activity of the sperm plasma membrane protein PH-20 enables sperm to penetrate the cumulus cell layer surrounding the egg. *J. Cell Biol.* **1994**, *125* (5), 1157–1163.
- (15) Zhou, C.; Kang, W.; Baba, T. Functional characterization of double-knockout mouse sperm lacking SPAM1 and ACR or SPAM1 and PRSS21 in fertilization. *J. Reprod. Dev.* **2012**, *58* (3), 330–337.
- (16) Kawano, N.; Kang, W.; Yamashita, M.; Koga, Y.; Yamazaki, T.; Hata, T.; Miyado, K.; Baba, T. Mice lacking two sperm serine proteases, ACR and PRSS21, are subfertile, but the mutant sperm are infertile in vitro. *Biol. Reprod.* **2010**, *83* (3), 359–369.
- (17) Cesari, A.; Monclus, M. L.; Tejón, G. P.; Clementi, M.; Fornes, M. W. Regulated serine proteinase lytic system on mammalian sperm surface: There must be a role. *Theriogenology* **2010**, *74* (5), 699–711.e5.
- (18) Honda, A.; Siruntawinetti, J.; Baba, T. Role of acrosomal matrix proteases in sperm-zona pellucida interactions. *Hum. Reprod. Update* **2002**, *8*, 405–412.
- (19) Isotani, A.; Matsumura, T.; Ogawa, M.; Tanaka, T.; Yamagata, K.; Ikawa, M.; Okabe, M. A delayed sperm penetration of cumulus layers by disruption of acrosin gene in rats. *Biol. Reprod.* **2017**, *97* (1), 61–68.
- (20) Netzel-Arnett, S.; Bugge, T. H.; Hess, R. A.; Carnes, K.; Stringer, B. W.; Scarman, A. L.; Hooper, J. D.; Tonks, I. D.; Kay, G. F.; Antalis, T. M. The glycosylphosphatidylinositol-anchored serine protease PRSS21 (testisin) imparts murine epididymal sperm cell maturation and fertilizing ability. *Biol. Reprod.* **2009**, *81* (5), 921–932.

- (21) Girouard, J.; Frenette, G.; Sullivan, R. Comparative proteome and lipid profiles of bovine epididymosomes collected in the intraluminal compartment of the caput and cauda epididymidis. *Int. J. Androl.* **2011**, *34* (Spt2), e475–e486.
- (22) Raymond, A. S.; Elder, B.; Ensslin, M.; Shur, B. D. Loss of SED1/MFG-E8 results in altered luminal physiology in the epididymis. *Mol. Reprod. Dev.* **2010**, *77* (6), 550–563.
- (23) Reilly, J. N.; McLaughlin, E. A.; Stanger, S. J.; Anderson, A. L.; Hutcheon, K.; Church, K.; Mihalas, B. P.; Tyagi, S.; Holt, J. E.; Eamens, A. L.; Nixon, B. Characterisation of mouse epididymosomes reveals a complex profile of microRNAs and a potential mechanism for modification of the sperm epigenome. *Sci. Rep.* **2016**, *6*, 31794.
- (24) Ohto, U.; Ishida, H.; Krayukhina, E.; Uchiyama, S.; Inoue, N.; Shimizu, T. Structure of IZUMO1-JUNO reveals sperm-oocyte recognition during mammalian fertilization. *Nature* **2016**, *534*, 566–569.
- (25) Bleil, J. D.; Wassarman, P. M. Mammalian sperm-egg interaction: Identification of a glycoprotein in mouse egg zona pellucidae possessing receptor activity for sperm. *Cell* **1980**, *20* (3), 873–882.
- (26) Kim, J.; Kwon, W. S.; Rahman, M. S.; Lee, J. S.; Yoon, S. J.; Park, Y. J.; You, Y. A.; Pang, M. G. Effect of sodium fluoride on male mouse fertility. *Andrology* **2015**, *3*, 544–551.
- (27) Sun, Z. L.; Niu, R. Y.; Wang, B.; Jiao, Z. B.; Wang, J. M.; Zhang, J. H.; Wang, S. L.; Wang, J. D. Fluoride-induced apoptosis and gene expression profiling in mice sperm in vivo. *Arch. Toxicol.* **2011**, *85* (11), 1441–1452.
- (28) Elbetieha, A.; Darmani, H.; Al-Hiyasat, A. S. Fertility effects of sodium fluoride in male mice. *Fluoride* **2000**, *33* (3), 128–134.
- (29) Izquierdo-Vega, J. A.; Sánchez-Gutiérrez, M.; Del Razo, L. M. Decreased in vitro fertility in male rats exposed to fluoride-induced oxidative stress damage and mitochondrial transmembrane potential loss. *Toxicol. Appl. Pharmacol.* **2008**, *230* (3), 352–357.
- (30) Lu, Z. J.; Wang, S. L.; Sun, Z. L.; Niu, R. Y.; Wang, J. D. In vivo influence of sodium fluoride on sperm chemotaxis in male mice. *Arch. Toxicol.* **2014**, *88* (2), 533–539.
- (31) Sullivan, R.; Mieusset, R. The human epididymis: Its function in sperm maturation. *Hum. Reprod. Update* **2016**, *22* (5), 574–587.
- (32) Zhou, W.; Deluiliis, G. N.; Turner, A. P.; Reid, A. T.; Anderson, A. L.; McCluskey, A.; McLaughlin, E. A.; Nixon, B. Developmental expression of the dynamin family of mechanoenzymes in the mouse epididymis. *Biol. Reprod.* **2017**, *96* (1), 159–173.
- (33) Akintayo, A.; Légaré, C.; Sullivan, R. Dicarboxyl-xylulose reductase (DCXR), a “moonlighting protein” in the bovine epididymis. *PLoS One* **2015**, *10* (3), e0120869.
- (34) Sharma, U.; Sun, F.; Conine, C. C.; Reichholz, B.; Kukreja, S.; Herzog, V. A.; Ameres, S. L.; Rando, O. J. Small RNAs Are Trafficked from the Epididymis to Developing Mammalian Sperm. *Dev. Cell* **2018**, *46* (4), 481–494.e6.
- (35) Eickhoff, R.; Baldauf, C.; Koyro, H. W.; Wennemuth, G.; Suga, Y.; Seitz, J.; Henkel, R.; Meinhardt, A. Influence of macrophage migration inhibitory factor (MIF) on the zinc content and redox state of protein-bound sulphhydryl groups in rat sperm: Indications for a new role of MIF in sperm maturation. *Mol. Hum. Reprod.* **2004**, *10* (8), 605–611.
- (36) Frenette, G.; Lessard, C.; Madore, E.; Fortier, M. A.; Sullivan, R. Aldose reductase and macrophage migration inhibitory factor are associated with epididymosomes and spermatozoa in the bovine epididymis. *Biol. Reprod.* **2003**, *69* (5), 1586–1592.
- (37) Martin-DeLeon, P. A. Epididymosomes: Transfer of fertility-modulating proteins to the sperm surface. *Asian J. Androl.* **2015**, *17* (5), 720–725.
- (38) Al-Dossary, A. A.; Strehler, E. E.; Martin-DeLeon, P. A. Expression and secretion of plasma membrane Ca^{2+} -ATPase 4a (PMCA4a) during murine estrus: Association with oviductal exosomes and uptake in sperm. *PLoS One* **2013**, *8* (11), e80181.
- (39) Boué, F.; Sullivan, R. Cases of human infertility are associated with the absence of P34H an epididymal sperm antigen. *Biol. Reprod.* **1996**, *54* (5), 1018–1024.
- (40) Baba, D.; Kashiwabara, S. I.; Honda, A.; Yamagata, K.; Wu, Q.; Ikawa, M.; Okabe, M.; Baba, T. Mouse sperm lacking cell surface hyaluronidase PH-20 can pass through the layer of cumulus cells and fertilize the egg. *J. Biol. Chem.* **2002**, *277* (33), 30310–30314.
- (41) Sano, K.; Gotoh, M.; Dodo, K.; Tajima, N.; Shimizu, Y.; Murakami-Murofushi, K. Age-related changes in cyclic phosphatidic acid-induced hyaluronic acid synthesis in human fibroblasts. *Hum. Cell* **2018**, *31* (1), 72–77.
- (42) Kimura, M.; Kim, E.; Kang, W.; Yamashita, M.; Saigo, M.; Yamazaki, T.; Nakanishi, T.; Kashiwabara, S.-i.; Baba, T. Functional roles of mouse sperm hyaluronidases, HYAL5 and SPAM1, in fertilization. *Biol. Reprod.* **2009**, *81* (5), 939–947.
- (43) Martin-DeLeon, P. A. Epididymal SPAM1 and its impact on sperm function. *Mol. Cell. Endocrinol.* **2006**, *250* (1), 114–121.
- (44) Evans, E. A.; Zhang, H.; Martin-DeLeon, P. A. SPAM1 (PH-20) protein and mRNA expression in the epididymides of humans and macaques: Utilizing laser microdissection/RT-PCR. *Reprod. Biol. Endocrinol.* **2003**, *1*, 54–65.
- (45) Belleannée, C.; Calvo, É.; Caballero, J.; Sullivan, R. Epididymosomes convey different repertoires of microRNAs throughout the bovine epididymis. *Biol. Reprod.* **2013**, *89* (2), 30.